



Investigation of age trends in tree-ring stable carbon and oxygen isotopes from northern Fennoscandia over the past millennium

Max Torbenson^{a,*}, Lara Klippel^b, Claudia Hartl^c, Frederick Reinig^a, Kerstin Treydte^d, Ulf Büntgen^{d,e,f,g}, Miroslav Trnka^{f,h}, Bernd Schöneⁱ, Lea Schneider^{j,k}, Jan Esper^{a,f}

^a Department of Geography, Johannes Gutenberg University, Mainz, Germany

^b Deutscher Wetterdienst (DWD), Offenbach am Main, Germany

^c Nature Rings – Environmental Research and Education, Mainz, Germany

^d Swiss Federal Institute for Forest, Snow and Landscape Research (WSL), Birmensdorf, Switzerland

^e Department of Geography, University of Cambridge, Cambridge, UK

^f Global Change Research Institute of the Czech Academy of Sciences (CzechGlobe), Brno, Czech Republic

^g Department of Geography, Faculty of Science, Masaryk University, Brno, Czech Republic

^h Department of Agrosystems and Bioclimatology, Faculty of Agronomy, Mendel University, Brno, Czech Republic

ⁱ Institute of Geosciences, Johannes Gutenberg University, Mainz, Germany

^j Department of Geography, Justus-Liebig-University, Giessen, Germany

^k Center for International Development and Environmental Research, Justus-Liebig-University, Giessen, Germany

ARTICLE INFO

Keywords:

Tree rings
Isotopes
Pinus sylvestris
Age trend
Fennoscandia

ABSTRACT

Although tree-ring stable carbon ($\delta^{13}\text{C}$) and oxygen ($\delta^{18}\text{O}$) isotopes are increasingly used for climate reconstructions, it remains unclear whether isotopic ratios from the two chemical elements and different tree species exhibit age-related trends that require removal prior to any paleoclimatic interpretation. Here, we present 2,355 $\delta^{13}\text{C}$ and 2,237 $\delta^{18}\text{O}$ decadal measurements of living and relict Scots pines (*Pinus sylvestris* L.) from northern Fennoscandia to investigate the occurrence of isotope-specific age trends at both the individual tree and chronology level between 941 and 2010 CE, together with total-ring width and maximum density data. We show that $\delta^{13}\text{C}$ values increase by $\sim 0.035\%$ per 10 years of tree age, and therefore require detrending, which is not the case for $\delta^{18}\text{O}$ that only contains minor changes related to age. This study provides independent evidence for the unique paleoclimatic value of stable $\delta^{18}\text{O}$ isotopic ratios from the cellulose of living and relict pine wood to reconstruct high- to low-frequency climate variability. Conversely, caution is advised when information from diverse tree-ring parameters, species and regions is combined in multi-proxy climate reconstructions.

1. Introduction

Tree-ring stable isotope (TRSI) records are increasingly used to assess past environmental changes. Due to the high cost and labor intensities, TRSI records are not as common as traditional tree-ring variables such as tree-ring width (TRW) or maximum latewood density (MXD). However, stable carbon ($\delta^{13}\text{C}$) and oxygen ($\delta^{18}\text{O}$) ratios have been shown to contain important information on past climatic conditions (e.g., Gagen et al., 2011; Hartl-Meier et al., 2015). Multi-centennial $\delta^{13}\text{C}$ and $\delta^{18}\text{O}$ chronologies have been used as predictors in reconstructions of drought (Büntgen et al., 2021; Kress et al., 2010; Labuhn et al., 2016), cloud cover (Helama et al., 2018; Loader et al., 2013; Young et al., 2012), sunshine hours (Hafner et al., 2014), temperature (Esper et al., 2015;

Szymczak et al., 2012; Treydte et al., 2009), relative humidity (Edwards et al., 2008; Haupt et al., 2011), and precipitation (Rinne et al., 2013; Treydte et al., 2006; Young et al., 2015). When used together with TRW or MXD data, isotope-based reconstructions can provide a more comprehensive understanding of the interaction between different climatological parameters (Linderholm et al., 2018; McCarroll and Loader, 2004). Joint analyses of past temperatures reconstructed from TRW and MXD (Esper et al., 2012a; McCarroll et al., 2013) with local and regional cloud cover reconstructions based on $\delta^{13}\text{C}$ measurements (Gagen et al., 2011; Loader et al., 2013; Young et al., 2012) have disentangled the coexistence of opposing cloud-cover temperature feedbacks at short- and long-term timescales in northern Fennoscandia and advanced our knowledge of cloud cover forcing (Young et al., 2019).

* Corresponding author.

E-mail address: mtorbens@uni-mainz.de (M. Torbenson).

<https://doi.org/10.1016/j.quaint.2022.05.017>

Received 21 March 2022; Received in revised form 18 May 2022; Accepted 26 May 2022

Available online 31 May 2022

1040-6182/© 2022 Elsevier Ltd and INQUA. All rights reserved.

Equally important, TRSIs may hold insights to certain spectral properties of climate variability that are omitted from other tree-ring proxies because of methodological limitations.

A source of uncertainty that continues to persist in dendroclimatic reconstructions is the challenging task of separating and retaining low-frequency climatic variability or trend (here considered representing timescales of one to several centuries) from non-climatic variance that is embedded in the tree-ring data. Age-related trends are inherent to TRW and MXD data and must be removed prior to climate analysis (Bräker, 1981; Cook and Peters, 1981), potentially resulting in loss of low-frequency variability. Even though methods have been developed to preserve the original ratio of high-to-low frequency variability (Briffa et al., 1992; Melvin & Briffa, 2008, 2014), most detrending approaches remove the low-frequency component intentionally as its interpretation is ambiguous (Cook et al., 1995; Esper et al., 2004). Some studies have suggested that isotopic ratios are not influenced by tree age and thus require no detrending (Büntgen et al., 2021; Gagen et al., 2007; Young et al., 2011), which would mitigate the loss of low-frequency variability in the standardization process. No agreement on this hypothesis exists, however.

There is a long line of studies on age trend in tree-ring $\delta^{13}\text{C}$, covering a wide range of tree species and study regions (for a comprehensive review see Leavitt, 2010). Lower $\delta^{13}\text{C}$ values during juvenile growth have been reported, yet the described depletion phase varies between 10- and 80-years following tree establishment (Bert et al., 1997; Daux et al., 2012; Duquesnay et al., 1998; Freyer, 1979; Gagen et al., 2008; McCarroll et al., 2020; Raffalli-Delerce et al., 2004; Saurer et al., 1995). Other studies outlining prolonged age trends throughout the trees' lifespan (Esper et al., 2010; Helama et al., 2015) or even a lack of such effects completely (Büntgen et al., 2021; Kilroy et al., 2016), further distort a conclusive assessment. Likewise, significant age-related trends have also been noted in $\delta^{18}\text{O}$ (Esper et al., 2010; Treydte et al., 2006; Yamada et al., 2018), but also the lack thereof (Büntgen et al., 2020; Nagavciuc et al., 2019). These disagreements may be due to differences in species and/or location but could also be a result of methodological choices involving series truncation prior to analysis (Gagen et al., 2011; Loader et al., 2013) or the pooling of samples (Lavergne et al., 2017; Leavitt, 2008; Szymczak et al., 2012; Xu et al., 2019). The extent of age-related trend or its absence becomes critically important in cases where tree-ring isotope chronologies are extended back in time through subfossil materials, for which only the innermost segments of trunks are available due to decay and weathering (Duffy et al., 2017).

Northern Fennoscandia houses some of the most important dendrochronological records globally, combining living and subfossil wood samples for the last millennia (e.g., Esper et al., 2012a; Linderholm et al., 2010). The resulting annually resolved temperature reconstructions have had significant implications for our understanding of long-term climate variability (e.g., Esper et al., 2012b). In respect to the application of TRSI of Scots pine (*Pinus sylvestris* L.) from the region, contrasting evidence exists on age-related trends in $\delta^{13}\text{C}$. Changes limited to the juvenile growth phase (Gagen et al., 2007) and trends throughout the life of trees (Helama et al., 2015) have been reported. A thorough analysis of trends in Fennoscandian $\delta^{18}\text{O}$ records has yet to be conducted.

Here we present a new collection of 70 $\delta^{13}\text{C}$ and 66 $\delta^{18}\text{O}$ measurement series of Scots pine from northern Fennoscandia, including both living and subfossil material covering the last millennium. The data are of annual and decadal resolution and were produced from trees with a heterogeneous age structure, as well as different germination and end dates. As such, they represent an ideal setup to assess potential effects of long-term biological trends on raw measurements of TRSI over a crucial period of climate variability and together with TRW and MXD measurements from the same trees, represent a comprehensive approach to long-term variability in tree growth. We investigate the temporal persistence, stability, and magnitude of trends in all four variables and identify varying age-related effects on these important paleoclimatic

proxies.

2. Materials and methods

2.1. Study site and tree-ring sample selection

In this study, we combine previously established TRW and MXD data from the N-SCAN network (Esper et al., 2012b) in the northern boreal forest biome of Finnish and Swedish Fennoscandia (Fig. 1a, Table 1) with newly produced $\delta^{13}\text{C}$ and $\delta^{18}\text{O}$ measurements of an N-SCAN subset. 59 ($\delta^{13}\text{C}$) and 55 ($\delta^{18}\text{O}$) subfossil pine trees collected in lakes at five sites were used to achieve a continuous replication and a heterogeneous age structure throughout the past millennium (Fig. 1b, Esper et al., 2016; Klesse and Frank, 2013). The subfossil data, spanning between 861 and 1891 CE, were complemented with $\delta^{13}\text{C}$ and $\delta^{18}\text{O}$ measurements from eleven living trees sampled during a more recent update of the N-SCAN network in 2010 and 2012. All subfossil disc samples were collected from submerged logs, while core samples were taken from living trees growing at the lake shore ensuring signal homogeneity (Hartl et al., 2021).

2.2. Sample measurements

All annual TRW and MXD data (covering 14,670 and 10,715 annual rings, respectively) were processed following standard techniques and derived from high-resolution density profiles using WALESCH X-ray radiographic techniques (Schweingruber et al., 1978; Björklund et al., 2019). Stable isotope measurements were performed following two varying approaches and temporal resolution. Isotope values of annual resolution were measured from whole wood ($n = 2,278$), and decadal resolved measurements ($n = 2,314$) were obtained from α -cellulose.

Isotope ratios of whole wood samples were measured for each tree separately at annual resolution (Fig. S1), from subfossil trunks of the late 9th to late 15th century CE. $\delta^{13}\text{C}$ measurements were obtained from ten subfossil trunks, and $\delta^{18}\text{O}$ measurements were obtained from nine subfossil trunks. Tree rings were separated with a razor blade under magnification and samples were milled using a Retsch ultra-centrifugal mill (Riechelmann et al., 2016). For $\delta^{13}\text{C}$ measurements, 1–2 mg and for $\delta^{18}\text{O}$ measurements 200–250 μg were weighed into tin foil capsules. The $\delta^{13}\text{C}$ samples were combusted in a Vario EL III elemental analyzer at 1150 °C and measured with an IsoPrime isotope ratio mass spectrometer (IRMS). The $\delta^{18}\text{O}$ samples were pyrolyzed in a high-temperature conversion elemental analyzer at 1450 °C, and values were obtained with an IsoPrime IRMS. The precision of measurements is $\pm 0.3\%$ for carbon and $\pm 0.5\%$ for oxygen.

Stable isotope ratios were measured on 10-year wood blocks (2001–2010, 1991–2000, ...) from eleven living and 49 ($\delta^{13}\text{C}$)/46 ($\delta^{18}\text{O}$) subfossil trees (Table 1). Thin sections were cut from the wood perpendicular to the fibers using a microtome (Gärtner and Nievergelt, 2010) before decadal blocks were split under magnification using a scalpel. The blocks were pulverized and homogenized using a Retsch ultra-centrifugal mill. The α -cellulose was extracted by removing resins, lignin, and other whole wood components with NaOH and NaClO₂ solutions (Loader et al., 2003). For $\delta^{13}\text{C}$, 0.85–0.95 mg cellulose (or alternatively 0.2–0.3 mg when the total sample amount was low) was packed into tin foil capsules and combusted to CO₂ using a EURO EA Elemental Analyzer. For $\delta^{18}\text{O}$, 200–250 μg cellulose was weighted into silver capsules and pyrolyzed to CO using an IsoPrime IRMS. The measurements precision is $\pm 0.3\%$ for carbon and $\pm 0.8\%$ for oxygen. All $\delta^{18}\text{O}$ ratios were measured in duplicates, with the arithmetic mean representing the final value. Isotope ratios are expressed as per mil deviations (‰) using the delta notation (δ) relative to Vienna Pee Dee Belemnite standard (VPDB - $\delta^{13}\text{C}$) and Vienna Standard Mean Ocean Water (VSMOW - $\delta^{18}\text{O}$) (Coplen, 1995; Craig, 1957).

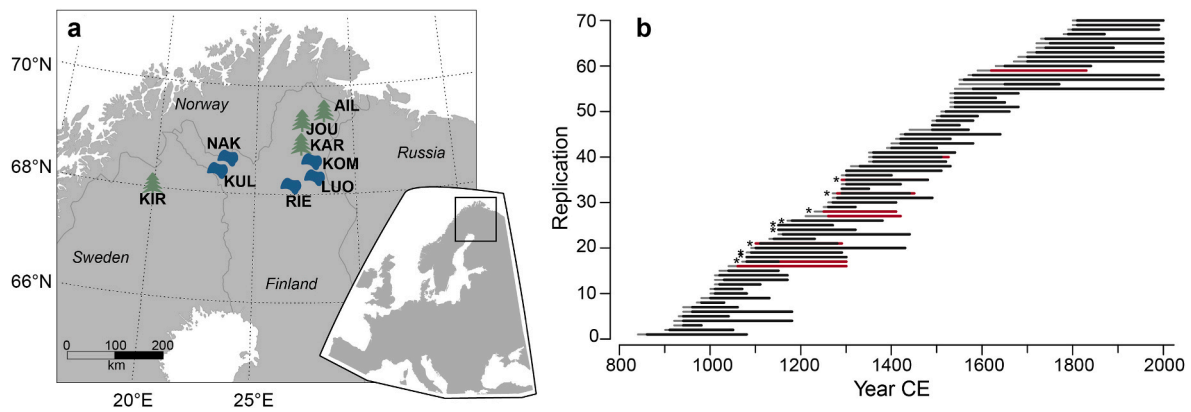


Fig. 1. Map of the sampling locations (a). Green symbols refer to sites with living trees and blue symbols to subfossil trees collected in lakes. Temporal coverage of 70 $\delta^{13}\text{C}$ and 66 $\delta^{18}\text{O}$ time series (b). Each black bar represents an individual sample where $\delta^{13}\text{C}$ and $\delta^{18}\text{O}$ measurements were performed, red bars denote additional $\delta^{13}\text{C}$ samples, grey bars indicate the estimated pith offset, and asterisks series with annual resolution. (For interpretation of the references to color in this figure legend, the reader is referred to the Web version of this article.)

Table 1
Site and data information.

	Site	Longitude	Latitude	No. Series				Period
		(°E)	(°N)	TRW	MXD	$\delta^{13}\text{C}$	$\delta^{18}\text{O}$	(CE)
Living	Ail	28.57	69.52	2	0	2	2	1701–2010
	Jou	27.40	69.26	2	0	2	2	1721–2010
	Kar	27.31	68.83	5	0	5	5	1561–2010
	Kir	20.03	67.95	2	0	2	2	1801–2000
Subfossil	Kom	28.00	68.50	20	20	20	18	861–1900
	Kul	23.00	68.50	14	14	14	14	981–1580
	Luo	28.00	68.50	9	9	9	7	1161–1880
	Näk	23.50	68.70	5	5	5	5	1011–1590
	Rie	26.56	68.16	11	11	11	11	941–1690
				70	59	70	66	

2.3. Data homogenization and chronology development

Annually resolved data were averaged for each decade to account for differences in temporal resolution by calculating 10-year means of the annual TRW and MXD measurements, as well as of the annually resolved $\delta^{13}\text{C}$ and $\delta^{18}\text{O}$ data. Offsets due to higher $\delta^{13}\text{C}$ and $\delta^{18}\text{O}$ values in α -cellulose, compared to whole wood, were handled by scaling the data of the subfossil whole wood samples to the mean and standard deviation of the data of the subfossil α -cellulose samples (Esper et al., 2005). Additionally, all values since 1850 CE were corrected for the industrial $\delta^{13}\text{C}$ decline known as the Suess effect (Keeling, 1979; Suess, 1955). We applied a mathematical correction scheme after Leuenberger (2007), in which $\delta^{13}\text{C}$ values can be expressed relative to the pre-industrial base value. We assume that for detection of age effects the use of different correction approaches (McCarroll et al., 2009; McCarroll and Loader, 2004; Treydte et al., 2009; Wang et al., 2011) is negligible because all germination predates 1820 CE (Fig. 1b) and the occurrence of significant differences among the corrections are reported to start in the 20th century (Köster et al., 2014). Negative exponential curves were fitted to individual $\delta^{13}\text{C}$ series and averaged to produce an alternative chronology.

Coherence between individual isotope series was assessed for each isotope variable using the mean inter-series correlation (R_{bar}) and the expressed population signal (EPS; Wigley et al., 1984). Coherence between $\delta^{13}\text{C}$ and $\delta^{18}\text{O}$ was assessed by calculating moving-window correlations between the decadal chronologies. Additionally, the resulting mean stable isotope chronologies were correlated with other regional tree-ring records.

2.4. Age trend analysis

Age trends were analyzed using individual series and the mean chronologies of all four tree ring parameters (TRW, MXD, $\delta^{13}\text{C}$, $\delta^{18}\text{O}$). Individual measurement series were normalized by subtracting the time series mean and then dividing the difference by the series' standard deviation (Z-transformed). The normalized series were aligned by biological age, taking into account the number of estimated rings absent to the first year of growth (pith offset) for each sample (Fig. 1b) determined at annual resolution subsequent to TRW measurements (Düthorn et al., 2013; Esper et al., 2012a). Age trends were assessed by fitting linear regressions through the arithmetic mean of all age aligned series, the so-called regional curve (Esper et al., 2003) and the significance of linear relationships was tested at $p \leq 0.05$ using a Mann-Kendall test (Kendall, 1975). Due to ranging autocorrelation in the data (Table S1), pre-whitened series were also tested to avoid spurious trends (Yue et al., 2002). The same procedure was performed over different time intervals using (i) 50-year regression windows and shifting these by one decade and (ii) windows of variable length with a sequential increase by ten years. The analysis started at a biological age of eleven due to low sample replication of $\delta^{13}\text{C}$ and $\delta^{18}\text{O}$ in the first ten years compared to the subsequent decades (8 vs. > 40 series) and to avoid the risk of a replication-induced trend distortion. As a result, the initial window only covers 40 years. Steepness of the slope was compared between TRW, MXD, $\delta^{13}\text{C}$ and $\delta^{18}\text{O}$, in windows of different lengths between the growth years 11–280 (the longest window for which overall $n \geq 5$).

3. Results

Substantial differences between whole wood and cellulose-based

isotope measurements were found with a mean offset of 1.3‰ and 4.3‰ for carbon and oxygen, respectively. These shifts are in line with previous reports (Loader et al., 2003; Riechelmann et al., 2016; Weigt et al., 2015). After adjusting the whole wood measurements for these differences, mean values for living trees ($\delta^{13}\text{C} = -24.70\text{‰}$, $\delta^{18}\text{O} = 24.88\text{‰}$) are not significantly different from those of subfossil trees (-24.99‰ and 24.88‰ respectively), suggesting that the subfossil material is not affected by any decay effects.

The mean segment lengths for the isotope records are 174 ($\delta^{13}\text{C}$, $n = 70$) and 166 ($\delta^{18}\text{O}$, $n = 66$) years. These results are therefore focused on the first 160/200 years of growth (individual series/mean respectively), for which replication is deemed robust ($n > 20$). Variance in the $\delta^{13}\text{C}$ measurements is higher than in $\delta^{18}\text{O}$ (Fig. 2) but the inter-series correlation is similar for both records, with notable changes present in both variables during the 16th century (Fig. 2c). Correlation between non-detrended $\delta^{13}\text{C}$ and $\delta^{18}\text{O}$ measurements of individual trees is positive, with mean $r = 0.48$ and median $r = 0.51$ (individual outliers range from $r = -0.42$ to 0.92). The correlation between non-detrended chronologies ($r = 0.57$ for the 941–2010 period) suggests significant independent variability in the two records, with two of thirds of the variance unexplained.

3.1. Individual series age trends

The majority of TRW series displays strong negative trends over their respective lifespans, as is the case for the vast majority of open-growing trees in the Northern Hemisphere mostly due to the diminishing relationship between circumference and volume (Cook and Peters, 1981). This decline in ring-width is, however, not present in all Scandinavian series, as competition and/or understory suppression likely hindered growth within the first 50–70 years. For these trees, the trend of growth within the initial 70 years is non-significant with a few TRW series indicating positive slopes, in contrast to the vast majority (Fig. 3e). Conversely, many MXD measurements display positive trend for the first decades of growth, but this change weakens, prior to becoming negative, and no significant trends are present beyond the 100-year mark. A larger portion of the individual MXD series display the same direction of slope as the mean MXD chronology, compared to individual and mean TRW series.

Over two-thirds of the raw $\delta^{13}\text{C}$ series display positive linear slopes over the maximum age window (Fig. 3g). The age-related trend is not apparent for the first two windows (11–50 and 11–60 years), but

significant trends are present for most trees from 11 to 70 years and beyond (e.g., 11–160). Few of the raw $\delta^{18}\text{O}$ series show any significant trends (positive or negative), with the exception for a limited number of series that display negative trends for the 11–50-year window. Even fewer display trend when considering windows beyond the 90-year biological age range (Fig. 3h). There is no increase in the number of series with a negative slope after the 50-year mark, which indicates a lack of long-term age-related effects after the tenth year of growth in $\delta^{18}\text{O}$.

3.2. Mean age trends

The linear change is -0.029 mm per decade over the first 200 years of growth after reversion of indices to TRW (Fig. 4a). As a result, the average ring after 200 years is less than half in width of that of years during the first decade of growth. A linear change of 0.02 g/cm³ per decade over the first 50 years of growth is found for the averaged MXD series. This increase is lost when regressing the first 200-year period and the slope is negative with a change of -0.001 g/cm³ per decade.

The mean regional curve of age-aligned $\delta^{13}\text{C}$ series suggests a clear age-related trend, with low values in biologically younger rings (Figs. 3g and 4c). Low values persist over the first 50 years of growth, and subsequently increase with age. Mean $\delta^{13}\text{C}$ values are -25.05‰ and -24.47‰ for the biological ages 1–50 and 111–250 years respectively (Fig. 3c). Linear regression fits to the regional curve over 50-year intervals demonstrate that changes of the mean are significant for the first 100 years of growth (Fig. 4e). Existing level offsets in $\delta^{13}\text{C}$ between young and older rings result in substantial slope changes throughout the trees' life spans (Fig. 4f). The age dependence corresponds to a linear change of 0.059‰ per decade over the first 100 years of growth and a change of 0.035‰ per decade for the first 200 years of growth (Fig. 4cf). Age effects are still present when limiting the comparison to the ten living trees (Fig. S2). The magnitude of age trend for the living trees is, however, slightly weaker compared to the average of the entire datasets (0.027‰ vs 0.035‰ per decade for the first 200 years of growth). No significant trend could be observed in the mean $\delta^{18}\text{O}$ regional curve over the initial 200 years (Fig. 4d), by values decreasing with -0.09‰ per century.

4. Discussion

The high sample replication and multi-parameter approach of this

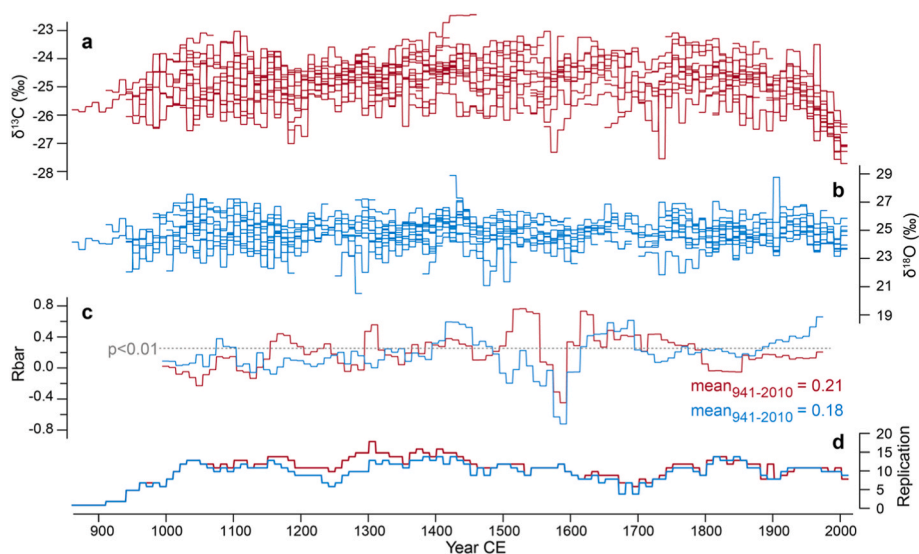


Fig. 2. Time series of 70 $\delta^{13}\text{C}$ (a) and 66 $\delta^{18}\text{O}$ (b) measurements of decadal resolution; 100-year moving Rbar (c) and sample replication (d) of $\delta^{13}\text{C}$ (red) and $\delta^{18}\text{O}$ (blue). (For interpretation of the references to color in this figure legend, the reader is referred to the Web version of this article.)

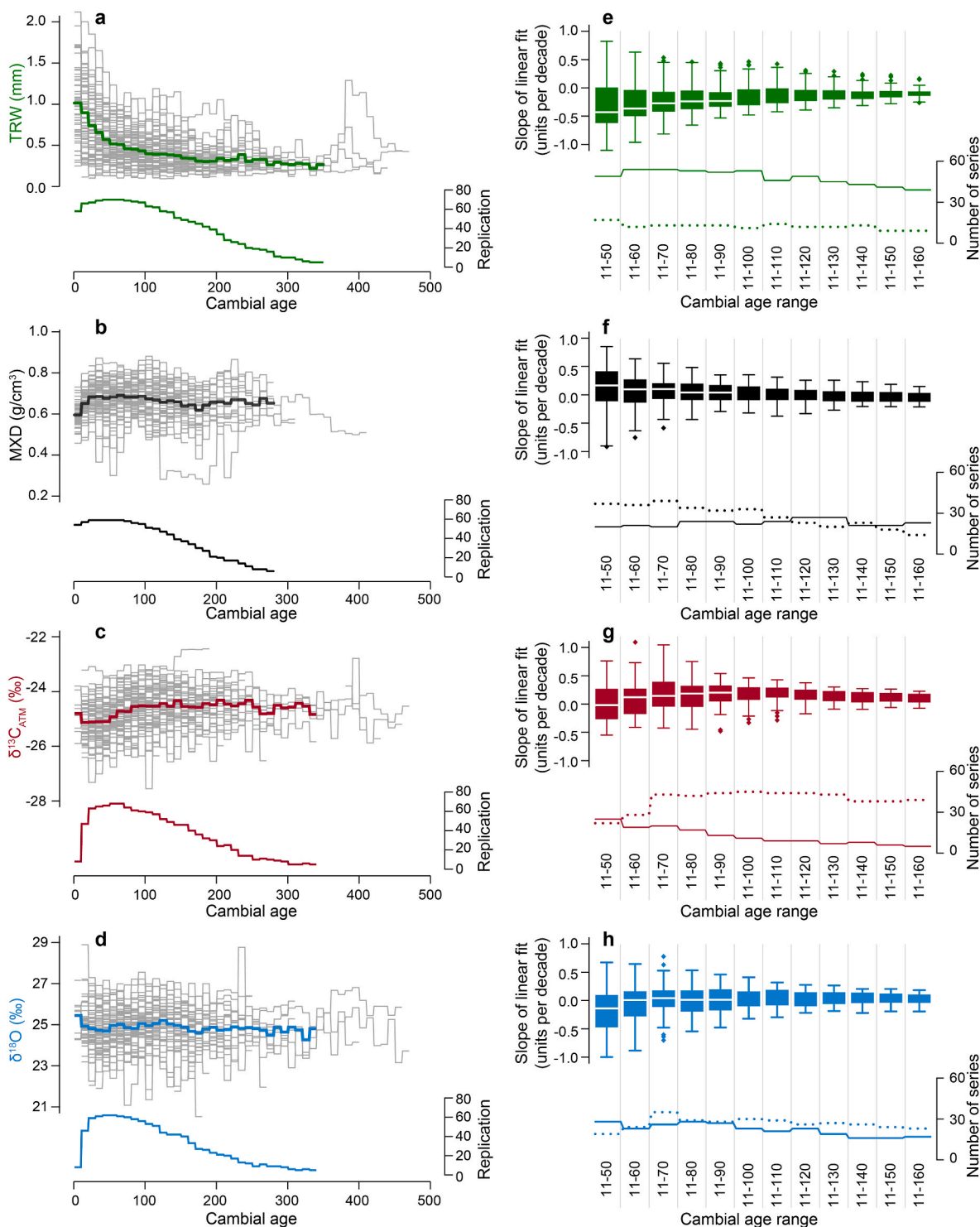


Fig. 3. Cambial age aligned time series (light grey) from 70 TRW (a), 59 MXD (b), 70 $\delta^{13}C_{ATM}$ (c), and 66 $\delta^{18}O$ (d) measurements. Colored lines in the upper panel of a-d indicate the arithmetic mean with $n \geq 5$ samples and colored lines in the lower panel the corresponding sample size. Single series age trend comparison of raw TRW (green, e), MXD (black, f), $\delta^{13}C_{ATM}$ (red, g) and $\delta^{18}O$ (blue, h) data. Boxplots (e-f) represent all slopes derived from age-aligned single series over the ring numbers 11–160 and slopes (per decade) are derived from least-square linear regressions through the age-aligned individual series. Linear regressions were fitted over different time intervals displayed as cambial age range classes (upper panels, e-f); the number of time series with a negative (solid line) or positive (dotted line) slope are shown in the bottom panels for each tree-ring parameter. (For interpretation of the references to color in this figure legend, the reader is referred to the Web version of this article.)

study provides important insight into age-related trends in Scots pine tree-ring variables from northern Fennoscandia. The greater effects of age on TRW than MXD measurements are in line with the scientific literature (e.g., Esper et al., 2012b; Grudd, 2008). The relatively low

Rbar calculated for both long isotope series (Fig. 2) is likely due to the decadal resolution of measurements, as evident by the significantly higher correlation values of the series that are annually resolved. However, this degradation of common signal among individual trees

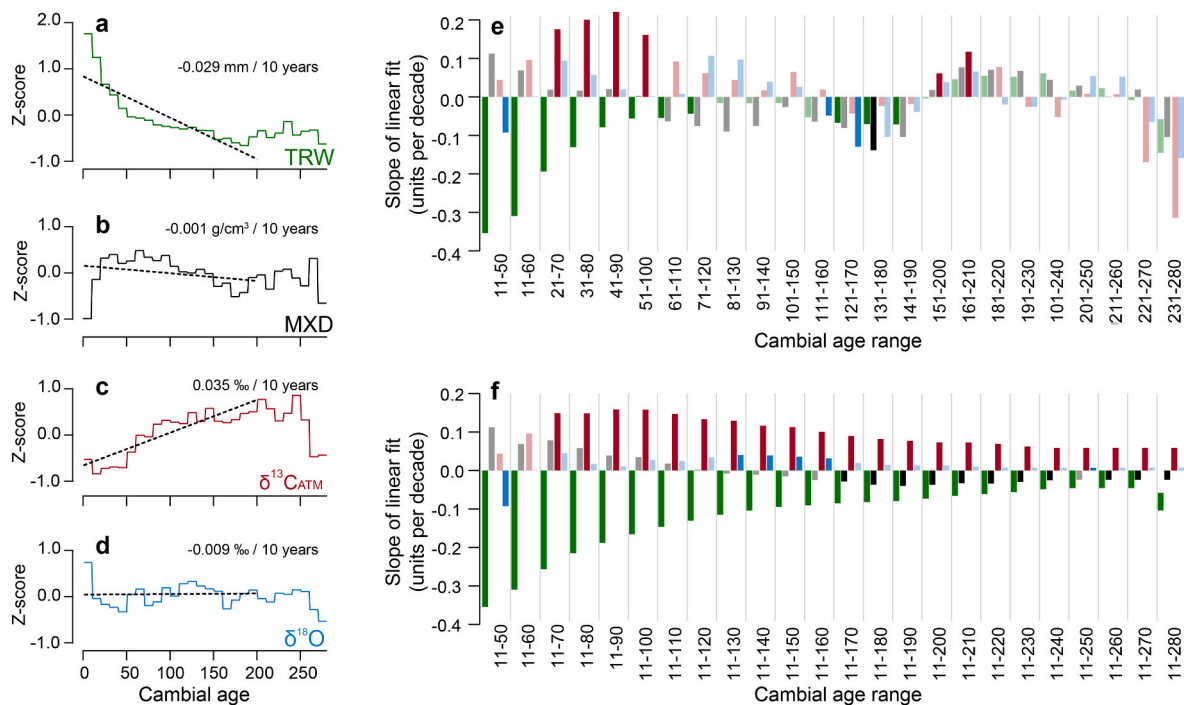


Fig. 4. Age trends in the mean regional curve of TRW (a); MXD (b); $\delta^{13}\text{C}_{\text{ATM}}$ (c); and $\delta^{18}\text{O}$ (d). The regional curves are based on Z-transformed individual series. Values displayed in (a–d) are changes in absolute units after back-transformation. Slope [per decade] derived from least-square linear regressions through the regional curves shown for: 50-year moving windows (e); and varying window lengths starting at the biological (estimated) age of 11 years (f). Shaded colors display non-significant and bold colors significant slopes at $p < 0.05$. (For interpretation of the references to color in this figure legend, the reader is referred to the Web version of this article.)

does not affect the results on age-related trends. The alignment of series, which was performed based on the absolutely dated and annually resolved TRW records, anchors all data to their biological age. Furthermore, the significant trends recorded for $\delta^{13}\text{C}$ (and likewise the lack of significant trends in $\delta^{18}\text{O}$) are beyond the length for which the decadal resolution of measurements could have an impact. As such, the information on age-related trends presented here should be considered as robust as if it was based on annually resolved measurements.

4.1. Fennoscandian stable isotope age trends in the context of previous studies

Our results on $\delta^{13}\text{C}$ age trends are in agreement with Helama et al. (2015), also studying Scots pine trees in northern Fennoscandia, for which the authors report persistent age-dependent trends in $\delta^{13}\text{C}$ and linear changes of 0.030‰–0.065‰ per decade. Gagen et al. (2007, 2008) and Young et al. (2011) attest juvenile effects in Scots pine over the first 50 years of growth but a lack of age signals beyond that period. Since these results (and the new data presented here) are of the same tree species and from the same study region, differences are likely related to varying measurement parameters: Gagen et al. (2007, 2008) and Young et al. (2011) processed latewood only for extraction of α -cellulose while Helama et al. (2015) considered cellulose from the whole ring. Presence or absence of trend is therefore unlikely to be dependent on changing proportions of the wood constituent, as our results are in line with those of Helama et al. (2015). A comparative study including all data from these studies is, however, needed to conclusively explain these differences.

Potential impacts of early/latewood use are suggested due to systematic seasonal variations in carbon isotope fractionation with an amplitude of around 2–3‰ (Helle and Schleser, 2004; Schulze et al., 2004), and age-related changes to early/latewood ratios could cause trend in isotopic values. While Gagen et al. (2007, 2008) and Young et al. (2011) focus on living trees only, Helama et al. (2015) restrict their

analysis to subfossil samples. Our approach is a combination of both living and subfossil trees, with no significant difference in absolute isotope values recorded between the two. Investigations further differ in their accuracy of pith-offset estimation and subsequently of the regional curve. Gagen et al. (2007) sampled felled trees, which allows for the precise development of a regional curve because no values need to be estimated towards the pith. Studies that use increment cores or partly rotten subfossil trunks require such estimates (Esper et al., 2003). Additionally, the sample size varies greatly among studies ($n = 12$ for Gagen et al., 2007; $n = 182$ for Helama et al., 2015; and $n = 70$ for this study). Although our results suggest that the $\delta^{13}\text{C}$ age trend is present when restricting the analysis to only living trees, roughly 25% of the series from the subfossil materials display negative (albeit non-significant) slopes. Consequently, the differences between results could be due to low sample sizes.

Studies on $\delta^{18}\text{O}$ are less numerous than for $\delta^{13}\text{C}$ and our results represent the most comprehensive analysis of age-related trends in Scots pine from northern Scandinavia. The only other available study attests to a lack of age-related trend but was limited to data for which the first 50 years of growth had been truncated (Young et al., 2011). Clear imprints of age trends in $\delta^{18}\text{O}$ records of other conifer species have, however, been recorded elsewhere. *Pinus uncinata* in the Spanish Pyrenees (Esper et al., 2010) and *Pinus cembra* in the Swiss Alps (Arosio et al.,), as well as juniper trees in northern Pakistan (Treydte et al., 2006), have been shown to contain negative trends and suggest that the absence or presence of such changes could be related to local/regional climatology. The occurrence of prolonged summer droughts and soil aridification in seasonally dry locations (such as Spain or Pakistan) increases evaporation in the topsoil layer. This process induces ^{18}O enrichment in surficial water, and therefore in cellulose, through enrichment in xylem and leaf water (Drake and Franks, 2003; Gangi et al., 2015; Hsieh et al., 1998). Furthermore, trees of different ages access more or less ^{18}O depleted soil water from different soil depths depending on the development of their root systems (Treydte et al., 2006; Hartl-Meier et al., 2015). Therefore, a

combination of both factors may also mitigate age-related trends in $\delta^{18}\text{O}$ in drought-prone environments. Conversely, the minor importance of leaf evapotranspiration, stomatal conductance, and soil evapotranspiration in humid conditions (McCarroll and Loader, 2004) may cause the absence of age trends in central Europe and Scandinavia, including the data presented here.

4.2. Recommendations and implications for low-frequency climate information

The retention of low-frequency signal variability remains one of the greatest challenges to dendroclimatic reconstruction exercises. If not limited by the same detrending constraints, isotope time-series from tree rings can offer additional spectral information to that gained from TRW and MXD. However, age-related trends in isotope records vary greatly across the world. These differences are likely due to a range of factors, including stand dynamics such as competition (Klesse et al., 2018), species-specific biochemical fractionation, and local climatology (e.g., McCarroll and Loader, 2004). Furthermore, methodological choices may influence the absence or presence of trend (Borella et al., 1999; Daux et al., 2018; Duffy et al., 2019). Pooling of measurements (Leavitt, 2010) and the truncation of data (Bégin et al., 2015; Labuhn et al., 2016; Loader et al., 2013) can make comparisons difficult, and low or temporally uneven sample sizes may further increase uncertainties. All these factors should be considered on a dataset-by-dataset basis, as is done with TRW and MXD, in order to maximize the potential of dendroisotope data in the reconstruction of pre-instrumental climate variability, and likewise, to limit misinterpretation of trend that may stem from non-climatic sources.

The $\delta^{18}\text{O}$ results presented here from Fennoscandian pine suggest a lack of age-related trend after the first 10 years of growth, and no application of standardization is deemed necessary. These data are therefore of key importance in exploring the multi-centennial to millennial-scale climatic trends that have been suggested elsewhere

(Esper et al., 2012b; Kaufman et al., 2009). Both isotope records display significant variability over the past millennium (Fig. 5abc), despite the decadal resolution of measurements.

The relationship between the two isotopic parameters remains relatively stable over the past 1,000 years (Fig. 5d). During the 13th century moving-window correlations ($m = 310$ years) between $\delta^{13}\text{C}$ and $\delta^{18}\text{O}$ decline, which could point to potential uncertainties associated with the combination of α -cellulose and whole wood samples. However, since the decline is still present when only using the α -cellulose samples, we assume additional imprints of a decoupling of otherwise co-varying forcings. The decline is greater for the detrended chronology, suggesting that the loss in correlation may be connected to low-frequency variability. Isotope series from northern Scandinavian pines have been shown to contain climate signals (e.g., Esper et al., 2018) and further work should focus on testing how these signals may be used to understand interactions between multiple climate variables (e.g., temperature and precipitation), over pre-historic times. Such analyses should, preferably, be based on annually resolved records.

Direct comparisons between the two stable isotope records presented here and other proxies or proxy-based reconstructions are constrained by the coarser temporal resolution. The relatively low inter-sample agreement, likely in part due to the 10-year averages, may further restrict such exercises. However, previous studies have highlighted the potential information that can be gained from tree ring-based isotope records at coarser resolution (Arosio et al.; Ziehm et al., 2018). The decadal $\delta^{13}\text{C}$ and $\delta^{18}\text{O}$ series presented here are significantly correlated with previous regional reconstructions when the latter are averaged in the same way, e.g., the non-detrended $\delta^{18}\text{O}$ chronology and the TRW chronology from Torneträsk (Melvin et al., 2013) display $r = 0.45$ for 941–2010 CE. Furthermore, the positive anomaly in the $\delta^{18}\text{O}$ chronology during early 15th century CE coincides with a warm period identified in previous studies from northern Sweden and Finland (e.g., Christiansen and Ljungqvist, 2011; Esper et al., 2012a). Although the purpose of this study is to assess the age-related trend in individual

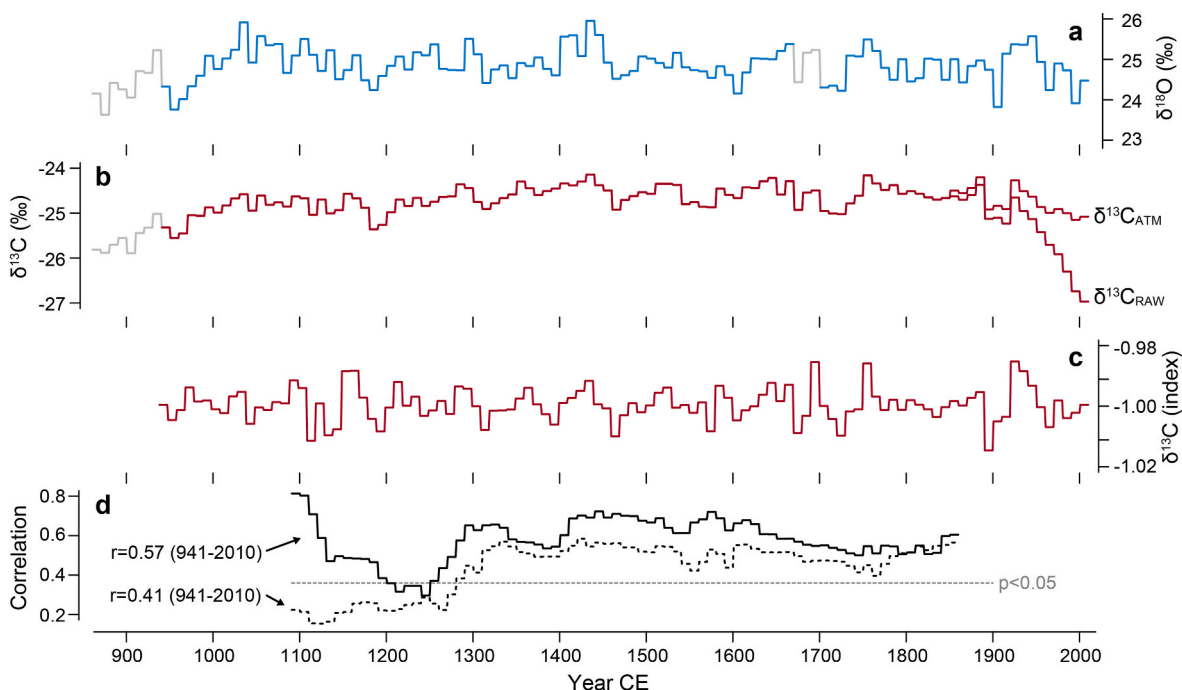


Fig. 5. Non-detrended tree-ring $\delta^{18}\text{O}$ (blue, a) and $\delta^{13}\text{C}$ (red, b) records (grey $n < 5$) plotted at decadal resolution. Corrections of the influence of decreasing atmospheric $\delta^{13}\text{C}$ values on tree-ring cellulose values due to fossil fuel burning ($\delta^{13}\text{C}_{\text{RAW}}$) were applied according to Leuenberger (2007) ($\delta^{13}\text{C}_{\text{ATM}}$) after CE 1850. Detrended (negative exponential) $\delta^{13}\text{C}_{\text{ATM}}$ chronology (c). 310-year moving inter-series correlation between non-detrended $\delta^{18}\text{O}$ and $\delta^{13}\text{C}_{\text{ATM}}$ chronologies (solid line) and between non-detrended $\delta^{18}\text{O}$ and detrended $\delta^{13}\text{C}_{\text{ATM}}$ chronologies (dotted line) over the period 941–2010 (d). (For interpretation of the references to colour in this figure legend, the reader is referred to the Web version of this article.)

isotope series from living and subfossil pine trees in Fennoscandia, the internal variability of the chronologies and the relationship with other records indicate that paleoclimate information could be extracted. Combined with the lack of trend related to biological age in the $\delta^{18}\text{O}$ series, we suggest that these records should be tested for new information on multi-centennial and millennium-scale climatic trends in the future.

5. Conclusions

The identification of potential age-related trends in TRSI time series and the removal of low-frequency noise is crucial prior to compiling mean chronologies for climate reconstruction. In this study we show that $\delta^{13}\text{C}$ series from Scots pine tree rings from northern Sweden and Finland exhibit significant changes with age, which require the application of statistical detrending prior to the use as a climate proxy as routinely performed with TRW and MXD measurements. Age trends range beyond the widely described juvenile phase of the first 50 years and remain present throughout the tree's lifespan, albeit weakened. In contrast, no indication for age-related trends in the $\delta^{18}\text{O}$ records beyond the juvenile phase were found in pines from Fennoscandia. Because there is no consensus about the potential mechanisms behind age-related trends in dendroisotope time series we recommend testing each site and species before further processing as is common practice for TRW and MXD data. Furthermore, we suggest that robust replication is required to assess the presence of age-related trend with confidence. The lack of any significant juvenile effect or persistent age trend suggests that the oxygen time series can be used reliably in paleoclimate analysis without any detrending or truncation of juvenile rings. $\delta^{18}\text{O}$ tree-ring records from northern Fennoscandia thus have the potential to retain climate information at all temporal frequencies, including multi-centennial periodicities.

Author contributions

J.E. conceived and planned the study, with feedback from L.S., U.B., C.H., and K.T.. L.K. performed the final analysis. All authors contributed to the interpretation of the findings. M.To. and F.R. assisted in the verification of results. M.To. and L.K. lead the writing of the manuscript with input from all other authors.

Data availability

The data that support the findings of this study will be made publicly available through the International Tree-Ring Databank (ITRDB) upon publication.

Declaration of competing interest

The authors declare that they have no known competing financial interests or personal relationships that could have appeared to influence the work reported in this paper.

Acknowledgments

The authors appreciate the constructive comments from three anonymous reviewers that helped improve the manuscript. We thank Elisabeth D uthorn for assistance during field work, Maria Mischel, Philipp R omer and Jutta Sonnberg for their help with the stable isotope measurements, and Dana Riechelmann for discussions of the results. K. T. acknowledges financial support by the Swiss National Science Foundation (SNF 200021_175888). C.H. was supported by the German Research Foundation [HA 8048/1-1]. J.E. was supported by the Gutenberg Research College. J.E., U.B., and M.To. acknowledge support by an ERC Advanced Grant Monostar(AdG 882727), J.E., U.B., and M. Tr. by SustES (CZ.02.1.01/0.0/0.0/16_019/0000797).

Appendix A. Supplementary data

Supplementary data to this article can be found online at <https://doi.org/10.1016/j.quaint.2022.05.017>.

References

- Arosio, T., Ziehmer, M.M., Nicolussi, K., Sch uchter, C., Leuenberger, M., 2020. Alpine Holocene tree-ring dataset: age-related trends in the stable isotopes of cellulose show species-specific patterns. *Biogeosciences* 17, 4871–4882. <https://doi.org/10.5194/bg-17-4871-2020>.
- B egin, C., Gingras, M., Savard, M.M., Marion, J., Nicaul, A., B egin, Y., 2015. Assessing tree-ring carbon and oxygen stable isotopes for climate reconstruction in the Canadian northeastern boreal forest. *Palaeogeogr. Palaeoclimatol. Palaeoecol.* 423, 91–101. <https://doi.org/10.1016/j.palaeo.2015.01.021>.
- Bert, D., Leavitt, S.W., Dupouey, J.-L., 1997. Variations of wood $\delta^{13}\text{C}$ and water-use efficiency of *Abies alba* during the last century. *Ecology* 78 (5), 1588–1596. [https://doi.org/10.1890/0012-9658\(1997\)078\[1588:VOWCAW\]2.0.CO;2](https://doi.org/10.1890/0012-9658(1997)078[1588:VOWCAW]2.0.CO;2).
- Bj orklund, J., von Arx, G., Nievergelt, D., Wilson, R., van den Bulcke, J., G unther, B., et al., 2019. Scientific merits and analytical challenges of tree-ring densitometry. *Rev. Geophys.* 57, 1224–1264. <https://doi.org/10.1029/2019RG000642>.
- Borella, S., Leuenberger, M., Saurer, M., 1999. Analysis of $\delta^{18}\text{O}$ in tree rings: wood-cellulose comparison and method dependent sensitivity. *J. Geophys. Res. Atmos.* 104 (D16), 19267–19273. <https://doi.org/10.1029/1999JD900298>.
- Br aker, O.U., 1981. Der Alterstrend bei Jahrringdichten und Jahrringbreiten von Nadelh olzern und sein Ausgleich. *Mitt. Forstl. Bundesversuchsanst. Wien* 142, 75–102.
- Briffa, K.R., Jones, P.D., Bartholin, T.S., Eckstein, D., Schweingruber, F.H., Karl en, W., et al., 1992. Fennoscandian summers from AD 500: temperature changes on short and long timescales. *Clim. Dynam.* 7 (3), 111–119. <https://doi.org/10.1007/BF00211153>.
- B untgen, U., Kol ar, T., Rybn icek, M., Ko nasov a, E., Trnka, M., A c, A., Krusic, P.J., Esper, J., Treydte, K., Reinig, F., Kiryanov, A., Herzig, F., Urban, O., 2020. No age trends in oak stable isotopes. *Paleoceanograph. Paleoclimatol.* 34 <https://doi.org/10.1029/2019PA003831>.
- B untgen, U., Urban, O., Krusic, P.J., Ryn icek Kol ar, T., Kyncl, T., et al., 2021. Recent European drought extremes beyond Common Era background variability. *Nat. Geosci.* 14, 190–196. <https://doi.org/10.1038/s41561-021-00698-0>.
- Christiansen, B., Ljungqvist, F.C., 2011. Reconstruction of the extratropical NH mean temperature over the last millennium with a method that preserves low-frequency variability. *J. Clim.* 24, 6013–6034. <https://doi.org/10.1175/2011JCLI4145.1>.
- Cook, E., Peters, K., 1981. The smoothing spline: a new approach to standardizing forest interior tree-ring width series for dendroclimatic studies. *Tree-Ring Bull.* 41, 45–53.
- Cook, E., Briffa, K.R., Meko, D.M., Graybill, D.A., Funkhouser, G., 1995. The “segment length curve” in long tree-ring chronology development for palaeoclimatic studies. *Holocene* 5 (2), 229–237. <https://doi.org/10.1177/095968369500500211>.
- Coplen, T.B., 1995. Discontinuance of SMOW and PDB. *Nature* 375 (6529). <https://doi.org/10.1038/375285a0>, 285–285.
- Craig, H., 1957. Isotopic standards for carbon and oxygen and correction factors for mass-spectrometric analysis of carbon dioxide. *Geochem. Cosmochim. Acta* 12 (1–2), 133–149. [https://doi.org/10.1016/0016-7037\(57\)90024-8](https://doi.org/10.1016/0016-7037(57)90024-8).
- Daux, V., Edouard, J.L., Masson-Delmotte, V., Stievenard, M., Hoffmann, G., Pierre, M., Mestre, O., Danis, P.A., Guibal, F., 2012. Can climate variations be inferred from tree-ring parameters and stable isotopes from *Larix decidua*? Juvenile effects, budmoth outbreaks, and divergence issue. *Earth Planet Sci. Lett.* 309, 221–233. <https://doi.org/10.1016/j.epsl.2011.07.003>.
- Daux, V., Michelot-Antalick, A., Lavergne, A., Pierre, M., Stievenard, M., Br eda, N., Damesin, C., 2018. Comparisons of the performance of $\delta^{13}\text{C}$ and $\delta^{18}\text{O}$ of *Fagus sylvatica*, *Pinus sylvestris*, and *Quercus petraea* in the record of past climate variations. *J. Geophys. Res.: Biogeosciences* 123 (4), 1145–1160. <https://doi.org/10.1002/2017JG004203>.
- Drake, P.L., Franks, P.J., 2003. Water resource partitioning, stem xylem hydraulic properties, and plant water use strategies in a seasonally dry riparian tropical rainforest. *Oecologia* 137 (3), 321–329. <https://doi.org/10.1007/s00442-003-1352-y>.
- Duffy, J.E., McCarroll, D., Barnes, A., Bronk Ramsey, C., Davies, D., Loader, N.J., et al., 2017. Short-lived juvenile effects observed in stable carbon and oxygen isotopes of UK oak trees and historic building timbers. *Chem. Geol.* 472, 1–7. <https://doi.org/10.1016/j.chemgeo.2017.09.007>.
- Duffy, J.E., McCarroll, D., Loader, N.J., Young, G.H.F., Davies, D., Miles, D., Bronk Ramsey, C., 2019. Absence of age-related trends in stable oxygen isotope ratios from oak tree rings. *Global Biogeochem. Cycles* 33, GB006195. <https://doi.org/10.1029/2019GB006195>.
- Duquesnay, A., Breda, N., Stievenard, M., Dupouey, J.L., 1998. Changes of tree-ring $\delta^{13}\text{C}$ and water-use efficiency of beech (*Fagus sylvatica* L.) in north-eastern France during the past century. *Plant Cell Environ.* 21 (6), 565–572. <https://doi.org/10.1046/j.1365-3040.1998.00304.x>.
- D uthorn, E., Holzk amper, S., Timonen, M., Esper, J., 2013. Influence of micro-site conditions on tree-ring climate signals and trends in central and northern Sweden. *Trees (Berl.)* 27 (5), 1395–1404. <https://doi.org/10.1007/s00468-013-0887-8>.
- Edwards, T.W.D., Birks, S.J., Luckman, B.H., MacDonald, G.M., 2008. Climatic and hydrologic variability during the past millennium in the eastern Rocky Mountains and northern Great Plains of western Canada. *Quat. Res.* 70 (2), 188–197. <https://doi.org/10.1016/j.yqres.2008.04.013>.

- Esper, J., Cook, E.R., Krusic, P.J., Peters, K., Schweingruber, F.H., 2003. Tests of the RCS method for preserving low-frequency variability in long tree-ring chronologies. *Tree-Ring Res.* 59 (2), 81–98.
- Esper, J., Frank, D.C., Wilson, R.J.S., 2004. Climate reconstructions: low-frequency ambition and high-frequency ratification. *Eos, Transactions Am. Geophys. Union* 85 (12), 113. <https://doi.org/10.1029/2004EO120002>.
- Esper, J., Frank, D.C., Wilson, R.J.S., Briffa, K.R., 2005. Effect of scaling and regression on reconstructed temperature amplitude for the past millennium. *Geophys. Res. Lett.* 32 (7), L07711 <https://doi.org/10.1029/2004GL021236>.
- Esper, J., Frank, D.C., Battipaglia, G., Büntgen, U., Holert, C., Treydte, K., et al., 2010. Low-frequency noise in $\delta^{13}\text{C}$ and $\delta^{18}\text{O}$ tree ring data: a case study of *Pinus uncinata* in the Spanish Pyrenees. *Global Biogeochem. Cycles* 24 (4), GB4018. <https://doi.org/10.1029/2010GB003772>.
- Esper, J., Büntgen, U., Timonen, M., Frank, D.C., 2012a. Variability and extremes of northern Scandinavian summer temperatures over the past two millennia. *Global Planet. Change* 88–89, 1–9. <https://doi.org/10.1016/j.gloplacha.2012.01.006>.
- Esper, J., Frank, D.C., Timonen, M., Zorita, E., Wilson, R.J.S., Luterbacher, J., et al., 2012b. Orbital forcing of tree-ring data. *Nat. Clim. Change* 2 (12), 862–866. <https://doi.org/10.1038/nclimate1589>.
- Esper, J., Konter, O., Krusic, P.J., Saurer, M., Holzschläger, S., Büntgen, U., 2015. Long-term summer temperature variations in the Pyrenees from detrended stable carbon isotopes. *Geochronometria* 42 (1). <https://doi.org/10.1515/geochr-2015-0006>.
- Esper, J., Krusic, P.J., Ljungqvist, F.C., Luterbacher, J., Carrer, M., Cook, E., et al., 2016. Ranking of tree-ring based temperature reconstructions of the past millennium. *Quat. Sci. Rev.* 145, 134–151. <https://doi.org/10.1016/j.quascirev.2016.05.009>.
- Esper, J., Holzschläger, S., Büntgen, U., Schöne, B., Keppler, F., Hartl, C., et al., 2018. Site-specific climatic signals in stable isotope records from Swedish pine forests. *Trees (Berl.)* 32 (3), 855–869. <https://doi.org/10.1007/s00468-018-1678-z>.
- Freyer, H.D., 1979. On the 13C record in tree rings. Part I. 13C Variations in northern hemispheric trees during the last 150 years. *Tellus* 31 (2), 124–137. <https://doi.org/10.3402/tellusa.v31i2.10417>.
- Gagen, M., McCarroll, D., Loader, N.J., Robertson, I., Jalkanen, R., Anchukaitis, K.J., 2007. Excursing the 'segment length curve': summer temperature reconstruction since AD 1640 using non-detrended stable carbon isotope ratios from pine trees in northern Finland. *Holocene* 17 (4), 435–446. <https://doi.org/10.1177/0959683607077012>.
- Gagen, M., McCarroll, D., Robertson, I., Loader, N.J., Jalkanen, R., 2008. Do tree ring $\delta^{13}\text{C}$ series from *Pinus sylvestris* in northern Fennoscandia contain long-term non-climatic trends? *Chem. Geol.* 252 (1–2), 42–51. <https://doi.org/10.1016/j.chemgeo.2008.01.013>.
- Gagen, M., Zorita, E., McCarroll, D., Young, G.H.F., Grudd, H., Jalkanen, R., et al., 2011. Cloud response to summer temperatures in Fennoscandia over the last thousand years: boreal cloud cover over the last millennium. *Geophys. Res. Lett.* 38 (5), L05701 <https://doi.org/10.1029/2010GL046216>.
- Gangi, L., Rothfuss, Y., Ogée, J., Wingate, L., Vereecken, H., Brüggemann, N., 2015. A new method for in situ measurements of oxygen isotopologues of soil water and carbon dioxide with high time resolution. *Vadose Zone J.* 14 (8) <https://doi.org/10.2136/vzj2014.11.0169> vzj2014.11.0169.
- Grudd, H., 2008. Torneträsk tree-ring width and density AD 500–2004: a test of climatic sensitivity and a new 1500-year reconstruction of north Fennoscandian summers. *Clim. Dynam.* 31, 843–857. <https://doi.org/10.1007/s00382-007-0358-2>.
- Gärtner, H., Nievergelt, D., 2010. The core-microtome: a new tool for surface preparation on cores and time series analysis of varying cell parameters. *Dendrochronologia* 28 (2), 85–92. <https://doi.org/10.1016/j.dendro.2009.09.002>.
- Hafner, P., McCarroll, D., Robertson, I., Loader, N.J., Gagen, M., Young, G.H., et al., 2014. A 520 year record of summer sunshine for the eastern European Alps based on stable carbon isotopes in larch tree rings. *Clim. Dynam.* 43 (3–4), 971–980. <https://doi.org/10.1007/s00382-013-1864-z>.
- Hartl, C., Dühorn, E., Tejedor, E., Kirchhefer, A.J., Timonen, M., Holzschläger, S., Büntgen, U., Esper, J., 2021. Micro-site conditions affect Fennoscandian forest growth. *Dendrochronologia* 65, 125787. <https://doi.org/10.1016/j.dendro.2020.125787>.
- Hartl-Meier, C., Zang, C., Büntgen, U., Esper, J., Rothe, A., Gottlein, A., et al., 2015. Uniform climate sensitivity in tree-ring stable isotopes across species and sites in a mid-latitude temperate forest. *Tree Physiol.* 35 (1), 4–15. <https://doi.org/10.1093/treephys/tpu096>.
- Haupt, M., Weigl, M., Grabner, M., Boettger, T., 2011. A 400-year reconstruction of July relative air humidity for the Vienna region (eastern Austria) based on carbon and oxygen stable isotope ratios in tree-ring latewood cellulose of oaks (*Quercus petraea* Matt. Liebl.). *Climatic Change* 105 (1–2), 243–262. <https://doi.org/10.1007/s10584-010-9862-1>.
- Helama, S., Arppe, L., Timonen, M., Mielikäinen, K., Oinonen, M., 2015. Age-related trends in subfossil tree-ring $\delta^{13}\text{C}$ data. *Chem. Geol.* 416, 28–35. <https://doi.org/10.1016/j.chemgeo.2015.10.019>.
- Helama, S., Arppe, L., Timonen, M., Mielikäinen, K., Oinonen, M., 2018. A 7.5 ka chronology of stable carbon isotopes from tree rings with implications for their use in palaeo-cloud reconstruction. *Global Planet. Change* 170, 20–33. <https://doi.org/10.1016/j.gloplacha.2018.08.002>.
- Helle, G., Schleser, G.H., 2004. Beyond CO₂-fixation by Rubisco – an interpretation of 13C/12C variations in tree rings from novel intra-seasonal studies on broad-leaf trees. *Plant Cell Environ.* 27, 367–380.
- Hsieh, J.C.C., Chadwick, O.A., Kelly, E.F., Savin, S.M., 1998. Oxygen isotopic composition of soil water: quantifying evaporation and transpiration. *Geoderma* 82 (1–3), 269–293. [https://doi.org/10.1016/S0016-7061\(97\)00105-5](https://doi.org/10.1016/S0016-7061(97)00105-5).
- Kaufman, D.S., Schneider, D.P., McKay, N.P., Ammann, C.M., Bradley, R.S., Briffa, K.R., et al., 2009. Recent warming reverses long-term arctic cooling. *Science* 325 (5945), 1236–1239. <https://doi.org/10.1126/science.1173983>.
- Kendall, M.G., 1975. *Rank Correlation Methods*. Griffin Press, London, UK.
- Keeling, C.D., 1979. The Suess effect: 13Carbon-14Carbon interrelations. *Environ. Int.* 2 (4–6), 229–300. [https://doi.org/10.1016/0160-4120\(79\)90005-9](https://doi.org/10.1016/0160-4120(79)90005-9).
- Kilroy, E., McCarroll, D., Young, G.H.F., Lo, N.J., Bale, R.J., 2016. Absence of juvenile effects confirmed in stable carbon and oxygen isotopes of European larch trees. *Acta Silvae et Ligni* 111, 27–33. <https://doi.org/10.20315/AselT.111.3>.
- Klesse, S., Frank, D., 2013. Testing the application of regional curve standardization to living tree datasets. In: Helle, G., Gärtner, H., Beck, W., Heinrich, I., Heußner, K.-W., Müller, A., Sanders, T. (Eds.), *Proceedings of the Dendrosymposium 2012 May 8th – 12th, 2012 in Potsdam and Eberswalde*, vol. 11. Potsdam: Helmholzgesellschaft, Germany, pp. 47–55.
- Klesse, S., Weigt, R., Treydte, K., Saurer, M., Schmid, L., Siegwolf, R.T.W., Frank, D.C., 2018. Oxygen isotopes in tree rings are less sensitive to changes in tree size and relative canopy position than carbon isotopes. *Plant Cell Environ.* 41 (12), 2899–2914. <https://doi.org/10.1111/pce.13424>.
- Konter, O., Holzschläger, S., Helle, G., Büntgen, U., Saurer, M., Esper, J., 2014. Climate sensitivity and parameter coherency in annually resolved $\delta^{13}\text{C}$ and $\delta^{18}\text{O}$ from *Pinus uncinata* tree-ring data in the Spanish Pyrenees. *Chem. Geol.* 377, 12–19. <https://doi.org/10.1016/j.chemgeo.2014.03.021>.
- Kress, A., Saurer, M., Siegwolf, R.T.W., Frank, D.C., Esper, J., Bugmann, H., 2010. A 350 year drought reconstruction from Alpine tree ring stable isotopes: isotope drought reconstruction. *Global Biogeochem. Cycles* 24 (2), GB2011. <https://doi.org/10.1029/2009GB003613>.
- Labuhn, I., Daux, V., Girardclos, O., Stievenard, M., Pierre, M., Masson-Delmotte, V., 2016. French summer droughts since 1326 CE: a reconstruction based on tree ring cellulose $\delta^{18}\text{O}$. *Clim. Past* 12 (5), 1101–1117. <https://doi.org/10.5194/cp-12-1101-2016>.
- Lavergne, A., Gennaretti, F., Risi, C., Daux, V., Boucher, E., Savard, M.M., et al., 2017. Modelling tree ring cellulose $\delta^{18}\text{O}$ variations in two temperature-sensitive tree species from North and South America. *Clim. Past* 13 (11), 1515–1526. <https://doi.org/10.5194/cp-13-1515-2017>.
- Leavitt, S.W., 2008. Tree-ring isotopic pooling without regard to mass: no difference from averaging $\delta^{13}\text{C}$ values of each tree. *Chem. Geol.* 252, 52–55. <https://doi.org/10.1016/j.chemgeo.2008.01.014>.
- Leavitt, S.W., 2010. Tree-ring C–H–O isotope variability and sampling. *Sci. Total Environ.* 408 (22), 5244–5253. <https://doi.org/10.1016/j.scitotenv.2010.07.057>.
- Leuenberger, M., 2007. To what Extent Can Ice Core Data Contribute to the Understanding of Plant Ecological Developments in the Past? In: Dawson, T.E., Siegwolf, R.T.W. (Eds.), *Isotopes as Indicators of Ecological Change, Terrestrial Ecology*. Academic Press, pp. 211–212. [https://doi.org/10.1016/S1936-7961\(07\)01014-7](https://doi.org/10.1016/S1936-7961(07)01014-7).
- Linderholm, H.W., Björklund, J.A., Seftigen, K., Gunnarson, B.E., Grudd, H., Jeong, J.-H., Drobyshev, I., Liu, Y., 2010. Dendroclimatology in Fennoscandia – from past accomplishments to future potential. *Clim. Past* 6, 93–114. <https://doi.org/10.5194/cp-6-93-2010>.
- Linderholm, H.W., Nicolle, M., Francus, P., Gajewski, K., Helama, S., Korhola, A., et al., 2018. Arctic hydroclimate variability during the last 2000 years: current understanding and research challenges. *Clim. Past* 14 (4), 473–514. <https://doi.org/10.5194/cp-14-473-2018>.
- Loader, N.J., Robertson, I., McCarroll, D., 2003. Comparison of stable carbon isotope ratios in the whole wood, cellulose and lignin of oak tree-rings. *Palaeogeogr. Palaeoclimatol. Palaeoecol.* 196 (3–4), 395–407. [https://doi.org/10.1016/S0031-0182\(03\)00466-8](https://doi.org/10.1016/S0031-0182(03)00466-8).
- Loader, N.J., Young, G.H.F., Grudd, H., McCarroll, D., 2013. Stable carbon isotopes from Torneträsk, northern Sweden provide a millennial length reconstruction of summer sunshine and its relationship to Arctic circulation. *Quat. Sci. Rev.* 62, 97–113. <https://doi.org/10.1016/j.quascirev.2012.11.014>.
- McCarroll, D., Loader, N.J., 2004. Stable isotopes in tree rings. *Quat. Sci. Rev.* 23 (7–8), 771–801. <https://doi.org/10.1016/j.quascirev.2003.06.017>.
- McCarroll, D., Gagen, M.H., Loader, N.J., Robertson, I., Anchukaitis, K.J., Los, S., et al., 2009. Correction of tree ring stable carbon isotope chronologies for changes in the carbon dioxide content of the atmosphere. *Geochim. Cosmochim. Acta* 73 (6), 1539–1547. <https://doi.org/10.1016/j.gca.2008.11.041>.
- McCarroll, D., Loader, N.J., Jalkanen, R., Gagen, M.H., Grudd, H., Gunnarson, B.E., et al., 2013. A 1200-year multiproxy record of tree growth and summer temperature at the northern pine forest limit of Europe. *Holocene* 23 (4), 471–484. <https://doi.org/10.1177/0959683612467483>.
- McCarroll, D., Duffy, J.E., Loader, N.J., Young, G.H.F., Davies, D., Miles, D., Bronk Ramsey, C., 2020. Are there enormous age-trends in stable carbon isotope ratios of oak tree rings? *Holocene* 30, 1637–1642. <https://doi.org/10.1177/0959683620941073>.
- Melvin, T.M., Briffa, K.R., 2008. A "signal-free" approach to dendroclimatic standardization. *Dendrochronologia* 26 (2), 71–86. <https://doi.org/10.1016/j.dendro.2007.12.001>.
- Melvin, T.M., Grudd, H., Briffa, K.R., 2013. Potential bias in 'updating' tree-ring chronologies using regional curve standardization: Re-processing 1500 years of Torneträsk density and ring-width data. *Holocene* 23 (3), 364–373. <https://doi.org/10.1177/0959683612460791>.
- Melvin, T.M., Briffa, K.R., 2014. CRUST: software for the implementation of regional chronology standardisation Part 1. Signal-free RCS. *Dendrochronologia* 32 (1), 7–20. <https://doi.org/10.1016/j.dendro.2013.06.002>.
- Nagavciuc, V., Ionita, M., Perşoiu, A., Popa, I., Loader, N.J., McCarroll, D., 2019. Stable oxygen isotopes in Romanian oak tree rings record summer droughts and associated

- large-scale circulation patterns over Europe. *Clim. Dynam.* 52, 6557–6568. <https://doi.org/10.1007/s00382-018-4530-7>.
- Raffalli-Delercq, G., Masson-Delmotte, V., Dupouey, J.L., Stievenard, M., Breda, N., Moisselin, J.M., 2004. Reconstruction of summer droughts using tree-ring cellulose isotopes: a calibration study with living oaks from Brittany (western France). *Tellus B* 56 (2), 160–174. <https://doi.org/10.3402/tellusb.v56i2.16405>.
- Riechelmann, D.F.C., Maus, M., Dindorf, W., Konter, O., Schöne, B.R., Esper, J., 2016. Comparison of $\delta^{13}\text{C}$ and $\delta^{18}\text{O}$ from cellulose, whole wood, and resin-free whole wood from an old high elevation *Pinus uncinata* in the Spanish central Pyrenees. *Isot. Environ. Health Stud.* 52 (6), 694–705. <https://doi.org/10.1080/10256016.2016.1161622>.
- Rinne, K.T., Loader, N.J., Switsur, V.R., Waterhouse, J.S., 2013. 400-year May–August precipitation reconstruction for Southern England using oxygen isotopes in tree rings. *Quat. Sci. Rev.* 60, 13–25. <https://doi.org/10.1016/j.quascirev.2012.10.048>.
- Saurer, M., Siegenthaler, U., Schweingruber, F., 1995. The climate-carbon isotope relationship in tree rings and the significance of site conditions. *Tellus B* 47 (3), 320–330. <https://doi.org/10.3402/tellusb.v47i3.16051>.
- Schulze, B., Wirth, C., Linke, P., Brand, W.A., Kuhlmann, I., Horna, V., Schulze, E.-D., 2004. Laser ablation-combustion-GC-IRMS - a new method for online analysis of intra-annual variation of ^{13}C in tree rings. *Tree Physiol.* 24 (11), 1193–1201. <https://doi.org/10.1093/treephys/24.11.1193>.
- Schweingruber, F.H., Fritts, H.C., Bräker, O.U., Drew, L.G., Schär, E., 1978. The X-ray technique as applied to dendroclimatology. *Tree-Ring Bull.* 38, 61–91.
- Suess, H.E., 1955. Radiocarbon concentration in modern wood. *Science* 122 (3166), 415–417. <https://doi.org/10.1126/science.122.3166.415-a>.
- Szymczak, S., Joachimski, M.M., Brauning, A., Hetzer, T., Kuhlemann, J., 2012. A 560 yr summer temperature reconstruction for the Western Mediterranean basin based on stable carbon isotopes from *Pinus nigra* ssp. *Laricio* (Corsica/France). *Clim. Past* 8, 1737–1749. <https://doi.org/10.5194/cpd-8-2111-2012>.
- Treydte, K., Schleser, G.H., Helle, G., Frank, D.C., Winiger, M., Haug, G.H., Esper, J., 2006. The twentieth century was the wettest period in northern Pakistan over the past millennium. *Nature* 440 (7088), 1179–1182. <https://doi.org/10.1038/nature04743>.
- Treydte, K., Frank, D.C., Saurer, M., Helle, G., Schleser, G.H., Esper, J., 2009. Impact of climate and CO_2 on a millennium-long tree-ring carbon isotope record. *Geochem. Cosmochim. Acta* 73 (16), 4635–4647. <https://doi.org/10.1016/j.gca.2009.05.057>.
- Wang, W., Liu, X., Shao, X., Leavitt, S., Xu, G., An, W., Qin, D., 2011. A 200 year temperature record from tree ring $\delta^{13}\text{C}$ at the Qaidam Basin of the Tibetan Plateau after identifying the optimum method to correct for changing atmospheric CO_2 and $\delta^{13}\text{C}$. *J. Geophys. Res.* 116 (G4), G04022 <https://doi.org/10.1029/2011JG001665>.
- Weigt, R.B., Bräunlich, S., Zimmermann, L., Saurer, M., Grams, T.E.E., Dietrich, H.-P., Siegwolf, R.T.W., Nikolova, P.S., 2015. Comparison of $\text{d}18\text{O}$ and $\text{d}13\text{C}$ values between tree-ring whole wood and cellulose in five species growing under two different site conditions. *Rapid Commun. Mass Spectrom.* 29, 2233–2244. <https://doi.org/10.1002/rcm.7388>.
- Wigley, T., Briffa, K.R., Jones, P.D., 1984. On the average of correlated time series, with applications in dendroclimatology and hydrometeorology. *J. Clim. Appl. Meteorol.* 23, 201–2013.
- Xu, G., Liu, X., Trouet, V., Treydte, K., Wu, G., Chen, T., et al., 2019. Regional drought shifts (1710–2010) in East Central Asia and linkages with atmospheric circulation recorded in tree-ring $\delta^{18}\text{O}$. *Clim. Dynam.* 52 (1–2), 713–727. <https://doi.org/10.1007/s00382-018-4215-2>.
- Yamada, R., Kariya, Y., Kimura, T., Sano, M., Li, Z., Nakatsuka, T., 2018. Age determination on a catastrophic rock avalanche using tree-ring oxygen isotope ratios - the scar of a historical gigantic earthquake in the Southern Alps, central Japan. *Quat. Geochronol.* 44, 47–54. <https://doi.org/10.1016/j.quageo.2017.12.004>.
- Young, G.H.F., Demmler, J.C., Gunnarson, B.E., Kirchhefer, A.J., Loader, N.J., McCarroll, D., 2011. Age trends in tree ring growth and isotopic archives: a case study of *Pinus sylvestris* L. from northwestern Norway. *Global Biogeochem. Cycles* 25 (2), GB2020. <https://doi.org/10.1029/2010GB003913>.
- Young, G.H.F., McCarroll, D., Loader, N.J., Gagen, M.H., Kirchhefer, A.J., Demmler, J.C., 2012. Changes in atmospheric circulation and the Arctic Oscillation preserved within a millennial length reconstruction of summer cloud cover from northern Fennoscandia. *Clim. Dynam.* 39 (1–2), 495–507. <https://doi.org/10.1007/s00382-011-1246-3>.
- Young, G.H.F., Loader, N.J., McCarroll, D., Bale, R.J., Demmler, J.C., Miles, D., et al., 2015. Oxygen stable isotope ratios from British oak tree-rings provide a strong and consistent record of past changes in summer rainfall. *Clim. Dynam.* 45 (11–12), 3609–3622. <https://doi.org/10.1007/s00382-015-2559-4>.
- Young, G.H.F., Gagen, M.H., Loader, N.J., McCarroll, D., Grudd, H., Jalkanen, R., et al., 2019. Cloud cover feedback moderates Fennoscandian summer temperature changes over the past 1,000 Years. *Geophys. Res. Lett.* 46 (5), 2811–2819. <https://doi.org/10.1029/2018GL081046>.
- Yue, S., Pilon, P., Phinney, B., Cavadas, G., 2002. The influence of autocorrelation on the ability to detect trend in hydrological series. *Hydrol. Process.* 16, 1807–1829. <https://doi.org/10.1002/hyp.1095>.
- Ziehmer, M.M., Nicolussi, K., Schlüchter, C., Leuenberger, M., 2018. Preliminary evaluation of tree-ring cellulose content as a novel supplementary proxy in dendroclimatology. *Biogeosciences* 15, 1047–1064. <https://doi.org/10.5194/bg-15-1047-2018>.